Journal of Power Sources 237 (2013) 187–194

Contents lists available at SciVerse ScienceDirect

Journal of Power Sources

journal homepage: www.elsevier.com/locate/jpowsour

Highly ordered graphene oxide paper laminated with a Nafion membrane for direct methanol fuel cells

C.W. Lin*, Y.S. Lu

Department of Chemical and Materials Engineering, National Yunlin University of Science and Technology, Douliu, Yunlin 640, Taiwan

HIGHLIGHTS

- A GO-laminated Nafion membrane for DMFC is originally proposed.
- The parallel orientation of the GO paper can effectively block methanol crossover.
- The novel membrane shows its superiority in DMFC at higher methanol feed concentrations.

ARTICLE INFO

Article history:
Received 9 January 2013
Received in revised form
26 February 2013
Accepted 1 March 2013
Available online 15 March 2013

Keywords:
Direct methanol fuel cell
Graphene oxide
Nafion membrane
Methanol permeability

ABSTRACT

This study presents graphene oxide (GO)-laminated Nafion 115 as a proton exchange membrane for a direct methanol fuel cell (DMFC). Compared to a GO-dispersed polymer composite membrane, a GO-laminated proton-conducting membrane is advantageous for DMFC operating at higher methanol feed concentrations. The novel laminate membrane consists of highly ordered GO paper with parallel orientation prepared by using a vacuum filtration method. This dual-layer membrane is fabricated by laminating the Nafion 115 membrane with a highly orientated GO paper through transfer printing followed by hot-pressing. Scanning electron microcopy (SEM) shows that the GO paper measuring approximately 1.0 μm thick (i.e., corresponding to 1.5 wt%) adhered well to the base membrane. The methanol permeability of the GO-laminated membrane is approximately 70% lower than that of Nafion 115 at an expense of a 22% decrease in proton conductivity. The proposed membrane has a 40% higher selectivity (i.e. ratio of proton conductivity to methanol permeability) than Nafion 115. The GO-laminated Nafion membrane is far superior to the pristine Nafion membrane in DMFC performance when operating at an 8 M methanol feed concentration.

1. Introduction

Direct methanol fuel cells (DMFC) are attractive power sources for a variety of applications because of their high energy density and simplicity [1]. However, several obstacles prevent the commercialization of DMFC. One of the main impediments is the non-availability of suitable proton conducting membranes. This is because current perfluorosulfonic acid membranes, such as Nafion membranes, have an unacceptably high rate of methanol crossover. This crossover wastes fuel and causes performance loss at the cathode through oxygen consumption and catalyst poisoning [2–4]. Consequently, plain Nafion is an inappropriate membrane for DMFC applications. Therefore, researchers are striving to develop suitable membranes with lower methanol permeability and reasonable proton conductivity.

Several studies have attempted to minimize the crossover of methanol through a membrane and maintain good proton conductivity [5–21]. Previous approaches include the synthesis of new membranes from polyhydrocarbon or perfluorinated materials [5–11], and the modification of existing Nafion membrane with various materials [12–21]. Among these two approaches, the second appear to be a promising method to achieve the desired properties. For example, Tricoli [12] reported that doping Nafion 117 with cesium cations significantly reduces its methanol permeability, and its proton conductivity decreases to a lesser extent. Palladium and palladium-alloy deposited Nafion membranes are effective in reducing methanol crossover [13–15]. Kim et al. [15] showed that Pd-impregnated nanocomposite Nafion membranes allow the selective transport of smaller water molecules or hydrogen ions, yet selectively inhibit the passage of larger methanol molecules. With this type of nanocomposite membrane, a DMFC can use a high concentration of methanol without significant power loss. A Nafion membrane modified with in-situ polymerized polypyrrole [16,17] or

* Corresponding author. Tel.: +886 5 534 2601x4613; fax: +886 5 531 2071.
E-mail addresses: lincw@yuntech.edu.tw, xj1222@yahoo.com.tw (C.W. Lin).

0378-7753/$ – see front matter © 2013 Elsevier B.V. All rights reserved.
http://dx.doi.org/10.1016/j.jpowsour.2013.03.005

polyaniline [18,19] has lower methanol permeability, and hence, enhances cell performance. The performance of Nafion/ORMOSIL membranes is superior to that of Nafion because of reduced methanol crossover [20,21]. Despite considerable work, the research on the modification of Nafion membranes remains active.

Graphene oxide (GO) is currently attracting considerable attention because of its potential applications in electronics and nanocomposites. GO is the product of the chemical exfoliation of graphite, and has been known for more than a century [22,23]. This oxide is essentially a graphene sheet derivatized by carboxylic acid at the edges and phenol hydroxyl and epoxide groups mainly on the basal plane [24]. Hydrophilic GO disperses readily in most polar solvents, such as water, breaking into macroscopic flakes that are mostly one layer thick. Pure GO is an electronic insulator with a differential conductivity between $1–5 \times 10^{-3}$ S cm^{-1} at a bias voltage of 10 V [25]. The potential advantages of using GO to improve the performance of a proton exchange membrane fuel cell (PEMFC) have recently been discovered, and have not been fully realized [26–32]. Ansari et al. [26] incorporated a small amount of GO in Nafion and found that it induces a significant degree of alignment in the ionic domains parallel to the film surface. Xu et al. [27] and Zarrin et al. [28] claimed that sulfonated GO can significantly improve polybenzimidazole and Nafion membrane performance for low humidity and high-temperature PEMFC performances. Cao et al. [29] reported a poly (ethylene oxide)/graphene oxide (PEO/GO) composite membrane aimed for low-temperature PEMFC. Hwang et al. [30] claimed that sulfonated polyimide (SPI)/GO membranes had higher proton conductivities than Nafion 117. Kumar et al. [31] were the first to evaluate GO paper as a polymer electrolyte for DMFC applications. However, their study shows that GO paper has a significantly higher methanol permeability of 18.2×10^{-6} cm^2 s^{-1} compared to Nafion 115, leading to a poor DMFC performance of 8 mW cm^{-2}. Choi et al. [32] investigated sulfonated GO (SGO)/Nafion composite membranes obtained from a highly homogenous solution of Nafion and SGO by solution casting. They evaluated the DMFC performance under 1 M methanol concentration on the anode side.

However, previous research has failed to explore the potential advantages of using GO to improve DMFC performance under higher methanol feed concentrations. Moreover, most studies adopted a similar approach of mixing a limited amount of GO with a base polymer, and then casting the mixture to form a GO-dispersed polymer composite membrane. This study proposes a merit approach to prepare a dual-layer laminate membrane that uses 2D GO paper as a methanol barrier for a DMFC operating at higher methanol feed concentrations. To demonstrate the merit of the currently proposed laminating approach, this study also presents a GO-dispersed poly(vinyl alcohol) (PVA) composite membrane prepared using the conventional mixing approach [26–30] for preliminary comparison.

2. Experimental

2.1. Materials

Graphite powders (crystalline, 300 mesh, 99%) was obtained from Alfa Aesar. Potassium permanganate (≥99%) was obtained from J.T. Baker. Sodium nitrate (≥99%) was purchased from Sigma–Aldrich. All reagents were used as received without further purification.

2.2. Preparation of highly ordered GO paper and GO-laminated Nafion membrane

GO was synthesized from the natural graphite powders using a modified Hummers and Offeman's method [33]. In brief, 1 g of graphite, 1 g of $NaNO_3$, and 46 mL of concentrated H_2SO_4 were mixed together and stirred in an ice bath for around 30 min. Then, 3 g of $KMnO_4$ was added slowly into the solution followed by stirring at 35 °C for 1 day to form thickened paste. Afterward 46 mL of de-ionized water was added slowly into the reaction solutions to avoid the reaction temperature rising to a limit of 98 °C. This solution was then kept stirring for 30 min. Finally, 140 mL of de-ionized water and 10 mL of H_2O_2 (30%) was poured into the mixture in sequence. This solution was then filtered by gravity filtration and the filter cake was washed with de-ionized water and 3% HCl solution alternatively. This filtered cake was then dispersed and washed with de-ionized water for several times by repeated centrifugation. The resulting samples were then dried by lyophilization to avoid the aggregation of GO during the drying process.

Highly ordered GO paper was made according to Ref. [34]. Colloidal solution of GO was prepared in water at a concentration of 2 mg mL^{-1} using an ultrasonic water bath. GO paper was made by filtration of the resulting colloid through a membrane filter (cellulose acetate membrane filter of 47 mm in diameter, 0.2 μm pore size) followed by air drying and the GO content equivalent to 1.5 wt % was then transfer printing onto a Nafion 115 (DuPont) membrane according to Ref. [35]. The obtained GO-laminated Nafion 115 membrane was then hot pressed at 120 °C to assure good adhesion between GO and the Nafion membrane.

2.3. Preparation of GO-dispersed composite membrane

GO-dispersed PVA composite membranes were prepared according to a mixing and casting method [26–30]. The PVA-based polymer is a well-investigated semi-interpenetrating network, namely XPVA, consisting of PVA, sulfosuccinic acid as a cross-linking agent (SSA, 70 wt% solution in water, Aldrich), and poly(-styrene sulfonic acid-co-maleic acid) (PSSA-co-MA, ratio of styrene sulfonic acid to maleic acid is 3/1, average MW = 20,000 g mol^{-1}; Aldrich) according to our previous work [36]. The loaded amount of GO in the composite membrane (i.e. namely GO-dispersed XPVA) is 0, 0.5, 1.0, 1.5, and 2.0 wt%, respectively.

2.4. Characterization of GO and composite membranes

Exfoliated GO sheet and GO-laminated Nafion membrane were firstly characterized using scanning electron microscopy (SEM, JXA-840, JEOL, Japan) and/or transmission electron microscopy (TEM, JEM-2100, JEOL, Japan). Exfoliated GO was extensively characterized by FT-IR spectrophotometer (Spectrum One, Perkin Elmer, USA) with a resolution of 4 cm^{-1} and 32 scans and X-ray diffraction (XRD) was carried out on an X-ray diffractometer (MiniFlex II, Rigaku, USA) using Cu Kα radiation ($\gamma = 0.15406$ nm). The diffraction patterns obtained in a scan range of 5°–100° were collected with a scan rate of 2° min^{-1}.

The water uptake (WU) of membrane was determined by measuring the change in the weight before and after the hydration. The membrane was immersed in deionized water for 24 h, and then surface-attached water onto the membrane was removed with filter paper. After that, the wetted membrane weight (W_{wet}) was determined as quickly as possible. Weight of dry membrane (W_{dry}) was determined after completely drying in vacuum at 60 °C for 48 h then at 100 °C for 1 h. The WU value was calculated by using the following equation.

$$\text{WU}\ (\%) = \frac{W_{wet} - W_{dry}}{W_{dry}} \times 100 \quad (1)$$

Titration method was used to determine the ion-exchange capacity (IEC). Each membrane sample was soaked in 50 mL of 1 M

sodium chloride aqueous solution overnight to exchange protons with sodium ions. The ion-exchanged solution was titrated with 0.005 M sodium hydroxide solution. The IEC value was then determined using the following equation.

$$\mathrm{IEC} = \frac{M_{i,\mathrm{NaOH}} - M_{f,\mathrm{NaOH}}}{W_{\mathrm{dry}}} = \frac{H^{+}(\mathrm{mmol})}{W_{\mathrm{dry}}} \quad (2)$$

where $M_{i,\ \mathrm{NaOH}}$ is the initial mmol of NaOH of titration and $M_{f,\ \mathrm{NaOH}}$ is the mmol (m_{eq}) of NaOH after equilibrium. H^{+} is the molar number of proton sites presented in the membrane, and W_{dry} is the weight (g) of the dry membrane.

Conductivity measurements were made at ambient temperature after equilibrating the membrane in deionized water for 24 h. Conductivities of fully hydrated membranes were measured by complex impedance analysis using Autolab PGSTST 30 instrument over a frequency range 70,000 Hz–100 Hz with ac perturbation of 5 mV. Stainless steel electrodes with 9.5 mm diameter were used as blocking electrodes. The resistance value associated with the membrane conductivity was determined from the high frequency intercept of the impedance with the real axis. The conductivity was calculated using the equation

$$\sigma = \frac{L}{R \cdot A} \quad (3)$$

where σ, L, R, and A denote the membrane conductivity, thickness of the membrane, the measured resistance on the membrane, and the cross-sectional area of the membrane perpendicular to current flow, respectively.

The methanol permeability of membrane was determined using a home-made side-by-side glass diffusion cell containing 3 wt% methanol solution in one side and pure water in the other side. The diffusion cell was maintained at a temperature of 35 °C. The different methanol concentrations between the two compartments caused a flux of methanol across the membrane. Methanol concentration within the water side was measured using gas chromatography (GC, China Chromatography 9800) at regular intervals. Methanol permeability was determined from the slope of the plot of methanol concentration in the receptor compartment versus time.

2.5. Single cell evaluation and electrochemical analysis

For a single cell performance test of DMFC, membrane electrode assemblies (MEA) were fabricated by using XPVA, GO-dispersed XPVA, Nafion 115, and GO-laminated Nafion 115 membrane respectively. Home-made electrodes prepared in the following manner have been utilized to fabricate MEA with 6.25 cm^2 active area by hot-pressing method. The cathode consisted of a Teflonized carbon cloth support, upon which a thin layer of uncatalyzed carbon bound with PTFE was coated homogeneously. Upon this diffusion layer, carbon supported Pt (50% Pt on carbon black, Alfa Aesar, USA) bound with Nafion was coated as catalyst layer to give a metal loading of 3 mg cm^{-2}. The anode was constructed using the same method except that the binder in the diffusion layer was Nafion instead of PTFE. Carbon supported Pt–Ru (58.1% Pt–Ru on Vulcan XC-72, E-TEK Division, De Nora North America, USA) was used as anode catalyst for DMFC. A thin layer of Nafion solution (0.6 mg cm^{-2} loading) was spread onto each electrode and dried in an oven at 80 °C for 2 h before hot-pressing. DMFC performance was evaluated in a cell test station by feeding methanol aqueous solution (2, 4, 6, 8 mol L^{-1}) to anode and oxygen gas to cathode. Methanol was fed at a fixed rate of 6 ml min^{-1} and oxygen at a gas flow rate of 100 SCCM. Electrochemical impedance spectra (EIS) analysis of the anodes was carried out at 2 mol L^{-1} methanol feeding, operating potential of 0.4 V, and frequency varied from 10,000 Hz–0.01 Hz. In this measurement, the cathode was fed with continuous hydrogen to serve as a dynamic hydrogen reference and counter electrodes. The methanol crossover rate of the fuel cell was measured by the

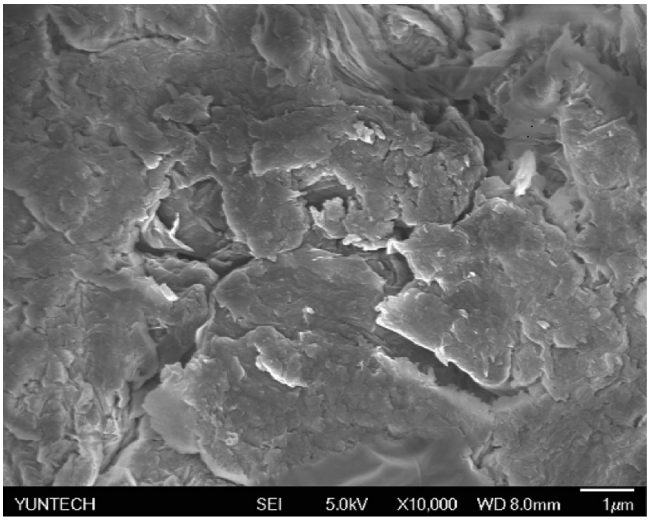

(a)

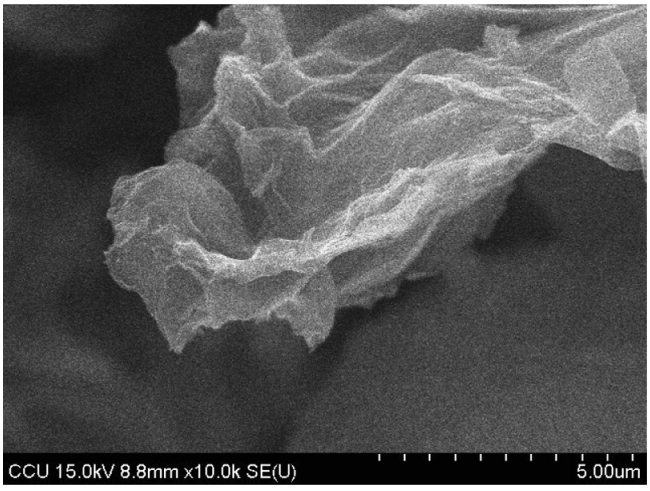

(b)

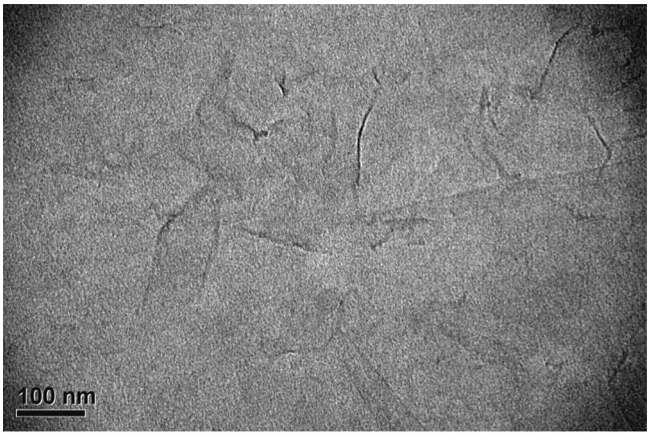

(c)

Fig. 1. (a) SEM image of graphite powers, (b) SEM image of graphene oxide, (c) TEM image of fully exfoliated graphene oxide sheet.

voltammetry method, with a scanning speed of 5 mV s^{-1} on the cathode (work electrode) and scanning range from 0.2 to 1.2 V. The work electrode was fed with nitrogen and the anode was supplied with 0.5 mol L^{-1} methanol aqueous solution to function as the counter and reference electrodes according to Ref. [37].

3. Results and discussion

3.1. Characterization of GO

Fig. 1(a) shows an SEM image of the commercial graphite powders obtained without further treatment. These starting powders exhibit a bundle- and flake-like morphology on the micrometer scale. After the oxidation process, Fig. 1(b) shows that the GO samples are completely exfoliated and exhibit curved and layer-like shapes with a smooth surface. The lateral size of the GO samples is within several micrometers. Fig. 1(c) shows a high resolution TEM image of the exfoliated GO sheets, which are somewhat wrinkled. This GO morphology is consistent with previous studies [38–40], which demonstrated that GO can undergo complete exfoliation in water under suitable conditions, yielding colloidal suspensions of almost entirely individual GO sheets.

XRD and FT-IR have been used to identify the features of the obtained GO sheets. The successful oxidation of graphite to GO can be confirmed by the FT-IR spectra because GO is a layered material consisting of hydrophilic oxygenated graphene sheets bearing oxygen functional groups on their basal planes and edges. Fig. 2 shows the changes occurring in the FT-IR spectrum of graphite after oxidation treatment. The FT-IR spectrum of GO exhibits several characteristic features, including the adsorption bands corresponding to carbonyl and carboxyl groups stretching at 1740 cm^{-1} and 1629 cm^{-1}, O–H deformation vibration at 1412 cm^{-1}, C–OH stretching at 1232 cm^{-1}, and C–O stretching at 1058 cm^{-1}, whereas no significant peak appeared in graphite. These results confirm the successful oxidation of graphite. Fig. 3 shows the XRD patterns of the GO sample and the precursor graphite. The peak at $2\theta = 26.5°$ in the graphite sample corresponds to the interplanar distance between the graphene layers. The layering in the GO paper is evident from its XRD pattern, in which the peak shifts from $2\theta = 26.5°$ to 11° corresponding to a layer-to-layer distance (d-spacing) of approximately 0.79 nm. The chemical oxidation of graphite disturbs the ordering of layers and introduces various functional groups (e.g., epoxide and carboxyl)

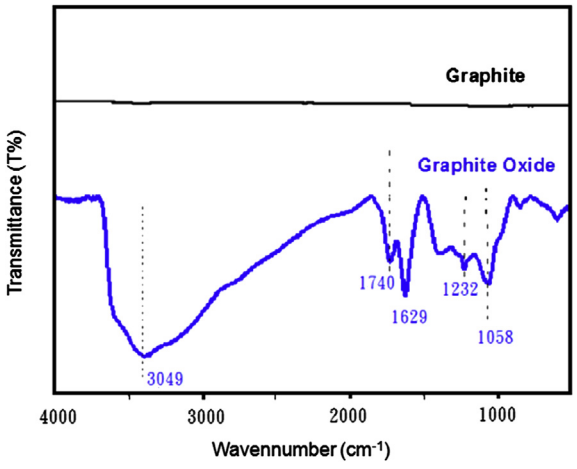

Fig. 2. FT-IR spectra of (a) original graphite, (b) graphene oxide.

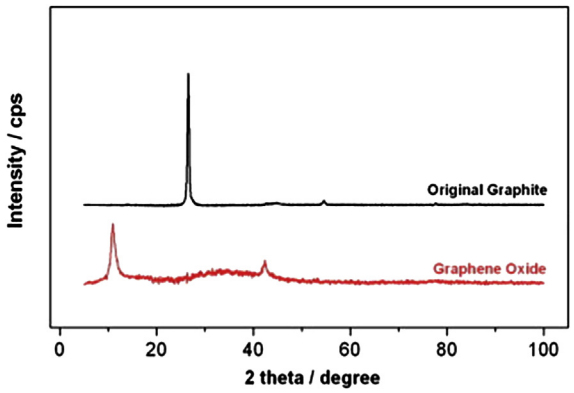

Fig. 3. XRD of (a) original graphite, (b) graphene oxide.

as the C–C bonds are broken during the oxidation process [41]. These functional groups increase the interplanar distance between the sheets and hence shift the XRD peak to a smaller angle of approximately 11°.

3.2. Properties of GO-dispersed XPVA composite membrane

To verify the advantages of incorporating GO into a polymeric matrix as a methanol barrier [30], this study presents a

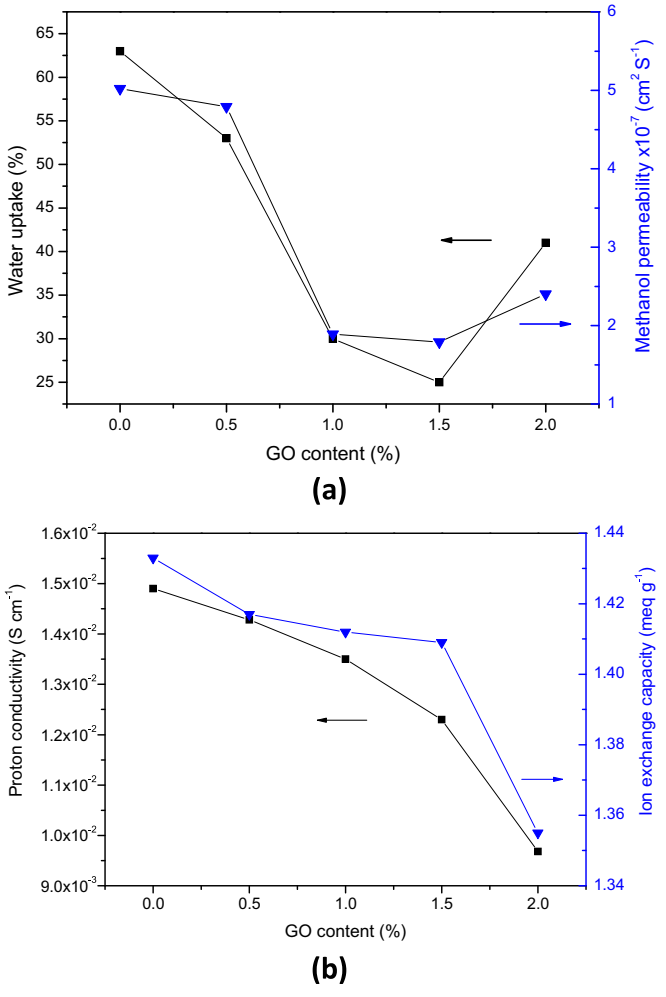

Fig. 4. WU, methanol permeability, proton conductivity, and IEC as a function of GO content.

preliminary experiment using a common approach based on a conventional mixing and casting method. Previous research [30] claimed that SPI/GO membranes have higher proton conductivities than Nafion. This study adopts an alternative GO-dispersed XPVA system for a preliminary study for two reasons. First, PVA material is more economical than Nafion solution. Second, the PVA-based proton conducting membranes used in a DMFC have been thoroughly studied [36,42,43]. Fig. 4(a) and (b) shows the associated properties of the GO-dispersed XPVA composite membrane. As can be seen in Fig. 4(a), the membrane reduces methanol permeability by as much as 64% at 1.5 wt% GO content. However, the methanol permeability turns upwards when the GO content reaches 2.0 wt%. With similar trend, the addition of hydrophilic GO largely reduces the water uptake of the membrane probably because of the interaction between the −COOH groups on the basal plane of the GO sheets and −OH groups within the PVA-based polymer matrix. Similar to the trend of methanol permeability, it turns upwards as GO content reaches to 2.0 wt%. This is likely because the highly hydrophilic nature of GO compensates for the lack of free volume caused by the GO-PVA interaction, dominating the water uptake and methanol permeability behaviors of the membrane. The reduction in water uptake may also be responsible for the slight loss of proton conductivity, as can be seen in Fig. 4(b). The proton conductivity appears to decrease slightly with the addition of GO because of the decreased effectiveness of GO as a proton moiety. Potentiometric acid–base titrations indicate that the presence of acidic sites on the basal plane of GO [44] enables GO to possess proton exchange capability. However, the IEC of the membrane also appears to decrease with the addition of GO. Among this series of the GO-dispersed XPVA membranes, the membrane with 1.5 wt% GO exhibits the greatest selectivity (i.e. proton conductivity/methanol permeability ratio), and therefore, was specifically selected for further evaluation in the DMFC test.

Fig. 5 shows a comparison of the polarization and power density curves of DMFC assembled with a pristine XPVA membrane and a GO-dispersed XPVA membrane, respectively. The tests were performed at 50 °C and a methanol feed concentration of 8 M. Because of the lower methanol permeability of the GO-dispersed XPVA membrane, the DMFC using this membrane has a slightly higher open circuit voltage (OCV) and power density than that of the pristine XPVA membrane. However, the improvement of the proton conducting membrane caused by the incorporation of GO is nearly imperceptible. This may be attributed to the lower proton conductivity and poor interface between the GO-dispersed XPVA membrane and the catalyst layer, which in turn leads to higher proton conducting resistance, and consequently, offsets the advantage of lower methanol permeability. Previous research [36] has shown that the DMFC performance of the XPVA-based MEA is as high as that of Nafion 115 membrane. In other words, a DMFC with a GO-dispersed XPVA membrane presumably does not overwhelm that with a Nafion 115 membrane. Therefore, this study turns to an alternative modification approach by laminating GO with a base membrane (i.e., Nafion 115 membrane) instead of dispersing it in a matrix. Because the XPVA membrane incorporated with 1.5 wt% GO appears to possess the best selectivity, this study adopts 1.5 wt% GO as a weight-loading basis for preparing GO-laminated Nafion membrane.

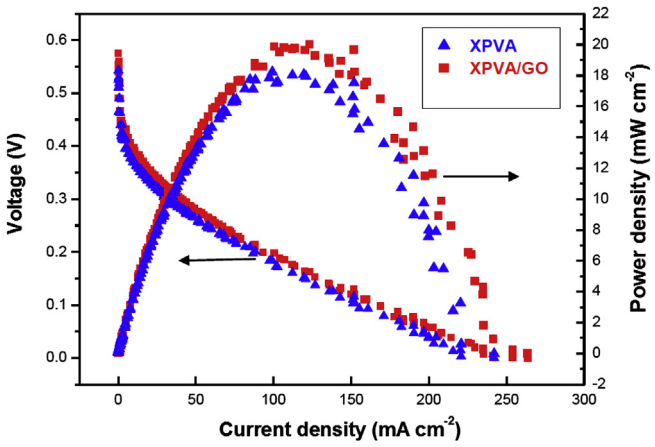

Fig. 5. Polarization and power density curves of DMFC operated at 50 °C and 8 M methanol feed concentration. The MEA were assembled with PVA membrane (▲) and GO-dispersed PVA membrane (■), respectively.

3.3. SEM of GO-laminated Nafion membranes

Previous research has shown that GO sheets can be assembled into a paper-like material under a directional flow [38–40]. Thus, the vacuum filtration of colloidal dispersions of GO sheets through a membrane filter (cellulose acetate membrane filter with a 47 mm diameter and 0.2 μm pore size) produces GO paper. After drying, the paper was subsequently coated on a Nafion membrane, resulting in a 1-μm-thick GO coating. Fig. 6(a) and (b) shows the GO-laminated Nafion membrane after the GO paper was transfer-printed onto the Nafion membrane at room temperature. When imaged using SEM, the fractured edges of the laminate sample showed well-packed layers of GO paper through almost the entire cross-section of the laminate. Hot-pressing treatment improved the interfacial bonding between the Nafion and the GO paper. Without proper hot-pressing treatment, the transferred GO paper disintegrated from the Nafion membrane when the laminate was immersed in water. Fig. 6(c) and (d) shows that the highly ordered GO paper retained its regular alignment in the laminate after the hot-pressing treatment, except for a slight reduction in thickness from 1.0 to approximately 0.8 μm.

3.4. Properties of GO-laminated Nafion membranes

3.4.1. Water uptake and IEC

Table 1 presents a comparison of both WU and IEC values for the GO-laminated Nafion 115 membrane and pristine Nafion 115 membrane. The GO-laminated Nafion membrane has a WU value of 10.28%, which is significantly lower than that of Nafion 115. Conversely, the GO-laminated Nafion membrane exhibited an IEC value of 0.99 meq g^{-1}, which is slightly greater than that of Nafion (0.89 meq g^{-1}). Because the sp^2-hybridized carbons on each sheet of GO paper contain carboxyl and carbonyl groups mostly at the sheet edges [38], GO and hydrophilic Nafion are highly compatible for the formation of a composite membrane. The Nafion membrane and the −COOH groups on the sheets of GO released H^+ ions when humidified, and the resulting laminate membrane might gain higher IEC. As Table 1 shows, the respective variation of WU and IEC for the GO-laminated Nafion shows a trend similar to those of a GO-dispersed Nafion nanocomposite electrolyte [28,32] prepared by mixing and casting. The variation in WU for the GO-laminated Nafion membrane is consistent with that of GO-dispersed Nafion membranes [28,32] and GO-dispersed XPVA membranes. The variation of IEC for the GO-laminated Nafion membrane is also consistent with that of GO-dispersed Nafion membranes. However, there is a discrepancy in IEC variation between a GO-dispersed Nafion membrane and a GO-dispersed PVA membrane. The incorporated GO has a positive effect in the first case, but a negative effect in the second. This discrepancy remains a controversy.

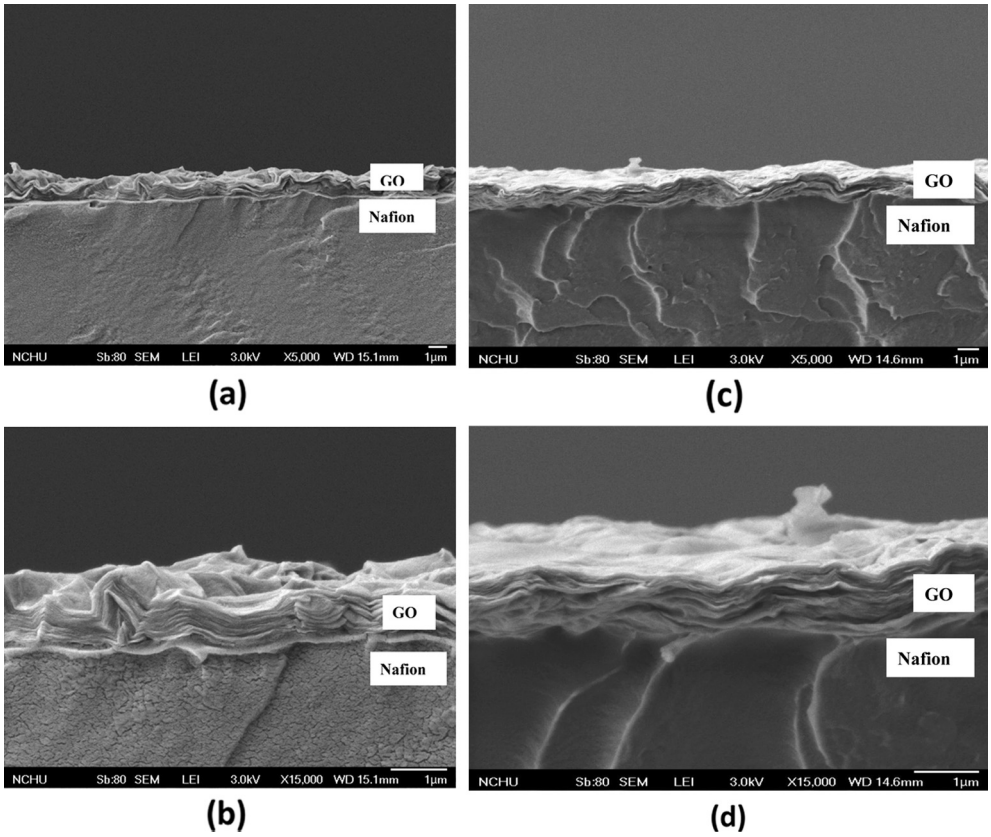

Fig. 6. SEM images of the GO-laminated Nafion membrane with different magnitudes. Prior hot-pressing: (a) X5000, (b) X15,000, and after hot-pressing: (c) X5000, (d) X15,000.

3.4.2. Proton conductivity and methanol permeability

The GO-laminated Nafion membrane has a proton conductivity of 2.35×10^{-2} S cm^{-1}, which is slightly lower than that of the Nafion 115 membrane (2.82×10^{-2} S cm^{-1}). Kumar et al. [31] reported that a membrane-electrode assembly (MEA) consisting of GO paper has a proton conductivity ranging from 4.1×10^{-2} S cm^{-1} to 8.2×10^{-2} S cm^{-1} at temperatures of 25–90 °C. Because GO is hydrophilic and is highly compatible for forming ionic-conducting composite membranes, the protons released from the COOH groups on the basal plane of GO sheets represent the key factor in the ionic conductivity of the GO portion of the laminate membrane. Certain reports [26,29] have shown that several GO-dispersed electrolyte membranes with limited GO loading have greater conductivities than their respective pristine membranes. However, Choi et al. [32] showed that incorporating GO into an electrolyte membrane produced no favorable improvement in proton conductivity. Thus, the effect of dispersed GO on the ionic conductivity of a proton-conducting membrane remains a controversy. This study shows that the GO-laminated Nafion membrane loses conductivity slightly.

Kumar et al. [31] also demonstrated that GO paper has a methanol permeability as high as 18.2×10^{-6} cm^2 s^{-1}. The Nafion 115 membrane in this study has a methanol permeability of 1.57×10^{-6} cm^2 s^{-1}, which is in good agreement with the literature [9]. Under the same test conditions, the proposed GO-laminated Nafion membrane has a methanol permeability of 0.928×10^{-6} cm^2 s^{-1}. An attempt to fabricate a neat GO [31] to measure its methanol permeability was performed. However, it failed because of the disintegration of GO paper in methanol solution during measurement. Thus, the decreased methanol crossover in the GO-laminated Nafion membrane may be attributable to the highly effective orientation of 2D GO sheets. This argument is supported by Paredes et al. [45], who indicated that, unlike water, methanol molecules are unable to penetrate the interlayer spaces of GO and disrupt the hydrogen bonds, which in turn prevents their exfoliation.

The GO-laminated Nafion membrane has a selectivity of 2.53×10^4 S cm^{-3} s, which is approximately 40% higher than that of Nafion 115. This higher selectivity suggests that the GO-laminated Nafion membrane can be used in a DMFC.

Table 1
Comparison of WU and IEC values of GO/Nafion composite membranes prepared by different approaches.

Membrane	The current work		Data from Ref. [32]		Data from Ref. [28]	
	WU [wt%]	IEC [meq g^{-1}]	WU [wt%]	IEC [meq g^{-1}]	WU [wt%]	IEC [meq g^{-1}]
Nafion	28.8	0.89	25.4	0.91	23	0.91
GO/Nafion	10.3	0.99	15.0	0.93	25	0.93

3.4.3. DMFC evaluation and electrochemical analysis

Fig. 7 shows a comparison of the DMFC performances of an MEA based on the GO-laminated Nafion membrane and the pristine Nafion 115 at various methanol feed concentrations (2, 4, 6, and 8 M) at 50 °C. Fig. 7(a) shows that a higher methanol concentration has a negative effect on the performance of the Nafion MEA, which suffers significant performance losses because of higher methanol crossover rates. Fig. 7(b) shows the polarization curves of the MEA based on the GO-laminated Nafion membrane. Unlike Nafion 115, the GO-laminated Nafion MEA achieved a maximum power density of 55 mW cm^{-2} with a 6 M methanol feed. Although the power density decreases to 32 mW cm^{-2} at an 8 M methanol feed concentration, its performance is still superior to a Nafion MEA under the same methanol feed concentration. To compare further the performance of the GO-laminated Nafion membrane and the

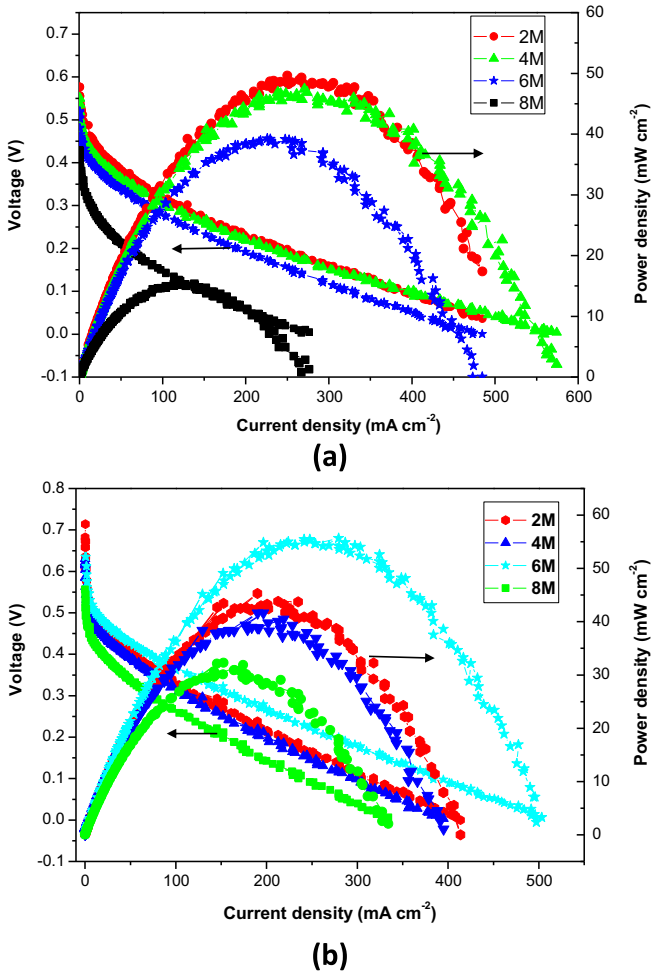

Fig. 7. Polarization curve and power density of DMFC assembled with (a) the Nafion 115, (b) the GO-laminated Nafion membrane.

pristine Nafion 115, Fig. 8 presents the respective polarization data for DMFC testing at 8 M and 50 °C. The peak power of the GO-laminated Nafion membrane is 100% higher than that of the Nafion 115 membrane. This clearly demonstrates the potential of the GO-laminated Nafion membrane for a DMFC operating at higher methanol feed concentrations.

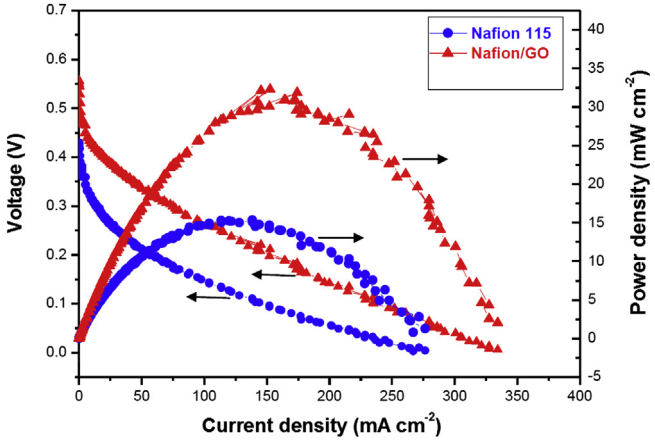

Fig. 8. Comparison of DMFC performances at 8 M methanol feed concentration by using Nafion 115 membrane (●) and GO-laminated Nafion membrane (▲).

This study uses impedance spectroscopy to investigate the effects of the interfacial behavior of the GO-laminated Nafion membrane on the MEA. The AC impedance approach offers certain distinct advantages over DC techniques. Fig. 9(a) shows the Nyquist plots of the Nafion 115 and the GO-laminated Nafion membranes at a frequency range of 10 kHz to 10 mHz. Except the membrane, all MEA components are identical. Therefore, the difference in the impedance spectra can be ascribed to the membrane and to the membrane/electrode interface. These plots consist of a loop reflecting inductive behavior. In this case, high fuel flow rates eliminated mass-transport limitations. In the high-frequency area, the intercepts with the real axis for the GO-laminated Nafion membrane and the pristine membrane are relatively close, indicating that lamination with GO on the anodic side of the Nafion membrane does not significantly increase the ionic ohmic drop and the interfacial resistance within the MEA. However, when compared to the pristine membrane, the GO-laminated membrane produces a greater low-frequency loop, reflecting a higher charge transfer resistance. In brief, the highly ordered GO paper on the anodic side can decrease the methanol crossover with only a slight decrease in electrolytic conductivity as compared to the Nafion 115 membrane. To verify this argument, this study also measured the electrochemical oxidation currents of both MEAs. In a conventional MEA, several methanol crossovers poison the anode catalyst as the

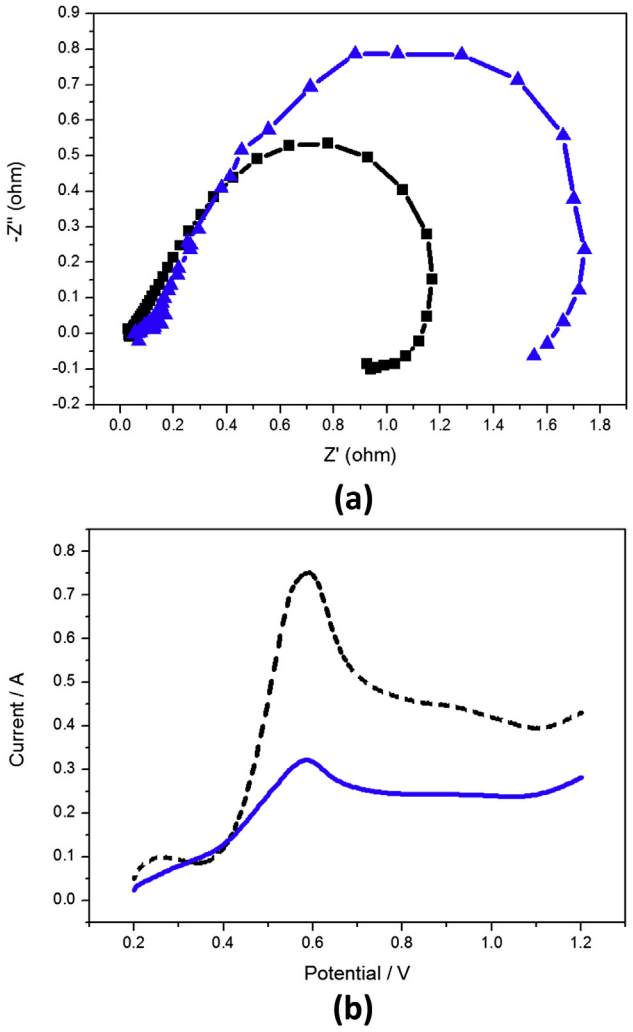

Fig. 9. (a) EIS spectra of the MEA with the Nafion 115 membrane (■) and the GO-laminated Nafion membrane (▲). (b) Methanol crossover curve of the MEA with the Nafion 115 membrane (dotted line) and the GO-laminated Nafion membrane (solid line).

methanol concentration increases. Fig. 9(b) shows a comparison of the methanol crossover rate for the fuel cell composed of the GO-laminated Nafion membrane and the pristine Nafion 115 membrane. Both types of MEA exhibit a peak oxidation current density at 0.6 V, which can be attributed to the methanol oxidation. The GO-laminated Nafion membrane exhibits a considerably smaller current peak than the pristine Nafion 115. This result indicates that the highly ordered GO-laminated layer facing anode helps prevent methanol crossover to the cathode. Therefore, the improved cell performance of the GO-laminated Nafion membrane can be attributed to high proton conductivity and low methanol crossover, which facilitate selective transport.

4. Conclusion

This study reports the preparation of highly ordered GO paper with parallel orientation using a vacuum filtration method, and subsequently, laminated Nafion 115 membrane through transfer printing and hot-pressing. The GO-laminated Nafion 115 membrane with a GO layer thickness of 0.8 μm has an IEC value of 0.99 meq g^{-1} and a proton conductivity of 2.35×10^{-2} S cm^{-1}. These values are close to those of the pristine Nafion 115 membrane. The methanol permeability of the proposed GO paper is 70% lower than that of Nafion 115 membrane, which is likely because the parallel orientation of the GO paper effectively decreases methanol crossover. Placing highly ordered GO paper on the surface of a Nafion membrane makes it easy to fabricate an MEA with good adhesion and suitable interface. The GO-laminated Nafion 115 membrane showed significantly higher DMFC performance than the pristine Nafion 115 at higher methanol feed concentration, displaying a peak power density of 55 mW cm^{-2} and 33 mW cm^{-2} at 6 and 8 M methanol feed, respectively (i.e., 38% and 100% higher than that of Nafion 115, respectively). This preliminary study presents a promising method to use GO sheets for preparing a methanol-inhibiting proton exchange membrane for DMFC. The proposed method is particularly suitable for DMFC operating at higher methanol feed concentrations.

Acknowledgment

Financial support from the National Science Council of Taiwan, ROC (under contract numbers 101-2221-E-224-066-MY3) is gratefully acknowledged.

References

[1] J.O.'M. Bockris, B.E. Conway, R.E. White (Eds.), Modern Aspects of Electrochemistry, Kluwer Academic Publishers/Plenum Press, NY, 2001, pp. 53–118.
[2] S. Wasmus, A. Kuver, J. Electroanal. Chem. 461 (1999) 14.
[3] S.R. Narayanan, T.I. Valdez, A. Kindler, C. Witham, S. Surampudi, H. Frank, Proceedings of the Fifteenth Annual Battery Conference on Applications and Advances, Long Beach, California, Institute of Electrical and Electronics Engineers, Piscataway, NJ, 2000, pp. 33–36.
[4] X. Ren, P. Zelency, S. Thomas, J. Davey, S. Gottesfeld, J. Power Sources 86 (2000) 111.
[5] J.A. Kerres, J. Memb. Sci. 185 (2001) 3.
[6] K.D. Kreuer, J. Memb. Sci. 185 (2001) 29.
[7] O. Savadogo, J. New Mater. Electrochem. Syst. 1 (1998) 47.
[8] M. Rikukawa, K. Sanui, Prog. Polym. Sci. 25 (2000) 1463.
[9] L. Li, J. Zhang, Y. Wang, J. Memb. Sci. 226 (2003) 159.
[10] N. Carretta, V. Tricoli, F. Picchioni, J. Memb. Sci. 166 (2000) 189.
[11] Y. Woo, S.Y. Oh, Y.S. Kang, B. Jung, J. Memb. Sci. 220 (2003) 31.
[12] V. Tricoli, J. Electrochem. Soc. 145 (1998) 3798.
[13] Z.Q. Ma, P. Cheng, T.S. Zhao, J. Power Sources 215 (2003) 327.
[14] W.C. Choi, J.D. Kim, S.I. Woo, J. Power Sources 96 (2001) 411.
[15] Y.M. Kim, K.W. Park, J.H. Choi, I.S. Park, Y.E. Sung, Electrochem. Commun. 5 (2003) 571.
[16] M.A. Smit, A.L. Ocampo, M.A. Espinosa-Medina, P.J. Sebastian, J. Power Sources 124 (2003) 59.
[17] E.B. Easton, B.L. Langsdrof, J.A. Hughes, J. Sultan, Z.G. Qi, A. Kaufman, P.G. Pickup, J. Electrochem. Soc. 150 (2003) 735.
[18] Q.M. Huang, Q.L. Zhang, H.L. Huang, W.S. Li, Y.J. Huang, J.L. Luo, J. Power Sources 184 (2008) 338–343.
[19] C.H. Wang, C.C. Chen, H.C. Hsu, H.Y. Du, C.P. Chen, J.Y. Hwang, L.C. Chen, H.C. Shih, J. Stejskal, K.H. Chen, J. Power Sources 190 (2009) 279–284.
[20] Y.J. Kim, W.C. Choi, S.I. Woo, W.H. Hong, J. Memb. Sci. 238 (2004) 213.
[21] C.W. Lin, K.C. Phan, R. Thangamuthu, J. Memb. Sci. 278 (2006) 437–446.
[22] O.D. Velev, K. Furusawa, K. Nagayama, Langmuir 12 (1996) 2374–2384.
[23] A. Boker, J. He, T. Emrick, T.P. Russell, Soft Matter 3 (2007) 1231–1248.
[24] J. Kim, L.J. Cote, F. Kim, W. Yuan, K.R. Shull, J. Huang, J. Am. Chem. Soc. 132 (2010) 8180–8186.
[25] D.R. Dreyer, S. Park, C.W. Bielawski, R.S. Ruoff, Chem. Soc. Rev. 39 (2010) 228–240.
[26] S. Ansari, A. Kelarakis, L. Estevez, E.P. Giannelis, Small 6 (2010) 205–209.
[27] C. Xu, Y.C. Cao, R. Kumar, X. Wu, X. Wang, K. Scott, J. Mater. Chem. 21 (2011) 11359–11364.
[28] H. Zarrin, D. Higgins, Y. Jun, Z. Chen, M. Fowler, J. Phys. Chem. C 115 (2011) 20774–20781.
[29] Y.C. Cao, C. Xu, X. Wu, X. Wang, L. Xing, K. Scott, J. Power Sources 196 (2011) 8377–8382.
[30] C.Y. Tseng, Y.S. Ye, M.Y. Cheng, K.Y. Kao, W.C. Shen, J. Rick, J.C. Chen, B.J. Hwang, Adv. Energy Mater. 1 (2011) 1220–1224.
[31] R. Kumar, M. Mamlouk, K. Scott, Int. J. Electrochem. 2011 (2011) 1–7.
[32] B.G. Choi, J. Hong, Y.C. Park, D.H. Jung, W.H. Hong, P.T. Hammond, H. Park, Nano 5 (2011) 5167–5174.
[33] W.S. Hummers Jr., R.E. Offeman, J. Am. Chem. Soc. 80 (6) (1958), 1339–1339.
[34] K.W. Putz, O.C. Compton, C. Segar, Z. An, S.T. Nguyen, L.C. Brinson, Nano 5 (8) (2011) 6601–6609.
[35] G. Eda, G. Fanchini, M. Chhowalla, Nat. Nanotechnol. 3 (2008) 270–274.
[36] C.W. Lin, Y.F. Huang, A.M. Kannan, J. Power Sources 171 (2007) 340.
[37] H. Tang, S. Wang, M. Pan, S.P. Jiang, Y. Ruan, Electrochim. Acta 52 (2007) 3714.
[38] S. Stankovich, D.A. Dikin, R.D. Piner, K.A. Kohlhaas, A. Kleinhammes, Y. Jia, Y. Wu, S.T. Nguyen, R.S. Ruoff, Carbon 45 (2007) 1558–1564.
[39] D.A. Dikin, S. Stankovich, E.J. Zimney, R.D. Piner, G.H.B. Dommett, G. Evmenenko, S.T. Nguyen, R.S. Ruoff, Nature 448 (2007) 457.
[40] G.I. Titelman, V. Gelman, S. Bron, R.L. Khalfin, Y. Cohen, H. Bianco-Peled, Carbon 43 (3) (2005) 641.
[41] H. He, J. Klinowski, M. Forster, A. Lerf, Chem. Phys. Lett. 287 (1998) 53–56.
[42] C.W. Lin, Y.F. Huang, A.M. Kannan, J. Power Sources 164 (2007) 449–456.
[43] Y.F. Huang, B.J. Hwang, C.W. Lin, J. Appl. Polym. Sci. 113 (1) (2008) 342–350.
[44] T. Szabo, E. Tombacz, E. Illes, I. Dekany, Carbon 2006 (44) (2006) 537–545.
[45] J.I. Paredes, S. Villar-Rodil, A. Martínez-Alonso, J.M.D. Tascón, Langmuir 24 (2008) 10560–10564.